Tunneling Nanoelectromechanical Switches Based on Compressible Molecular Thin Films

Farnaz Niroui,[†] Annie I. Wang,[†] Ellen M. Sletten,[‡] Yi Song,[†] Jing Kong,[†] Eli Yablonovitch,[§] Timothy M. Swager,[‡] Jeffrey H. Lang,[†] and Vladimir Bulović*,[†]

[†]Department of Electrical Engineering and Computer Science and [‡]Department of Chemistry, Massachusetts Institute of Technology, Cambridge, Massachusetts 02139, United States and [§]Department of Electrical Engineering and Computer Science, University of California, Berkeley, California 94720, United States

ABSTRACT Abrupt switching behavior and near-zero leakage current of nanoelectromechanical (NEM) switches are advantageous properties through which NEMs can outperform conventional semiconductor electrical switches. To date, however, typical NEMs structures require high actuation voltages and can prematurely fail through permanent adhesion (defined as stiction) of device components. To overcome these challenges, in the present work we propose a NEM switch, termed a "squitch," which is designed to electromechanically modulate the tunneling current through a nanometer-scale gap defined by an organic molecular film sandwiched between two electrodes. When voltage is applied across the electrodes, the generated electrostatic force compresses the sandwiched molecular layer, thereby reducing the tunneling gap and causing an exponential increase in the current through the device. The presence of the molecular layer avoids direct contact of the electrodes during the switching process. Furthermore, as the layer is compressed, the increasing surface adhesion forces are balanced by the elastic restoring force of the deformed molecules which can promote zero net stiction and recoverable switching. Through numerical analysis, we demonstrate the potential of optimizing squitch design to enable large on–off ratios beyond 6 orders of magnitude with operation in the sub-1 V regime and with nanoseconds switching times. Our preliminary experimental results based on metal–molecule–graphene devices suggest the feasibility of the proposed tunneling switching mechanism. With optimization of device design and material engineering, squitches can give rise to a broad range of low-power electronic applications.

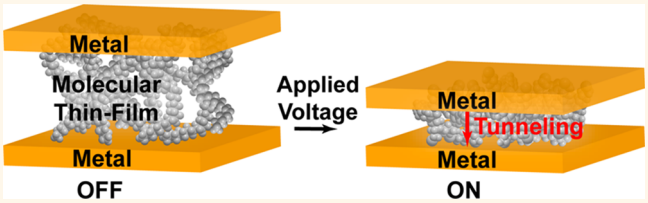

KEYWORDS: nanoelectromechanical (NEM) switches · stiction · organic molecular thin film · self-assembled monolayer · quantum tunneling · Simmons model · graphene

Nanoelectromechanical (NEM) switches have attracted increasing attention for ultralow power electronics applications, as they offer abrupt switching behavior with larger on–off ratios and near-zero off-state leakage currents compared to solid-state silicon complementary metal-oxide-semiconductor (CMOS) technologies.[1−8] Unfortunately, most NEM switches require relatively high actuation voltages (>1 V) and commonly suffer from device failure due to irreversible contact adhesion, defined as stiction.[1,9−12] In a typical NEM switch, a movable electrode is electrostatically attracted toward an opposing stationary electrode until direct contact is established, thereby turning on the switch. When the applied electrostatic force is released, the elastic restoring force provided by the deflected active electrode should break the contact, turning off the switch. However, if the adhesion force of the contacting electrodes exceeds the spring restoring force, the two electrodes will remain in contact resulting in permanent stiction and device failure (Figure 1a). Miniaturization of the gap between the electrodes often increases adhesion problems, but such gap reduction is necessary to reduce the NEM operating voltage in order to compete with the lower switching energies of state-of-the-art CMOS technologies. Previous studies have reported the use of self-assembled monolayers (SAMs) of low surface energy materials as antistiction coatings in electromechanical devices, lowering the surface adhesion forces upon contact and thus the possibility of stiction (Figure 1b).[13] In this paper, we propose a new approach to utilizing molecular layers in NEM switches based on metal–molecule–metal (MMM) switching gaps with a potential to minimize stiction (Figure 1c),

* Address correspondence to bulovic@mit.edu.

Received for review October 20, 2014 and accepted June 6, 2015.

Published online August 05, 2015
10.1021/acsnano.5b02476

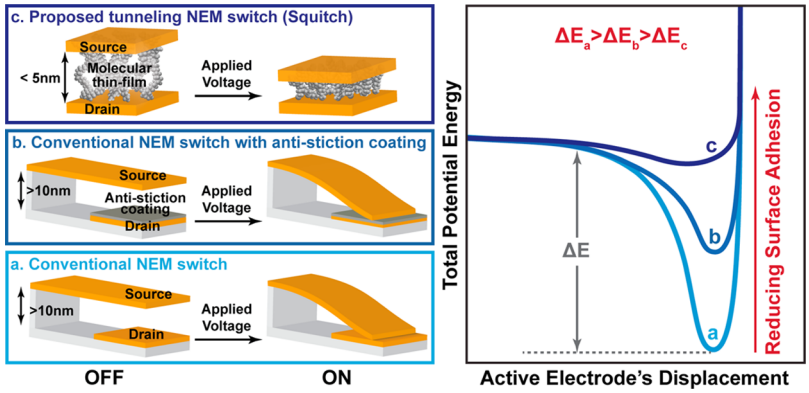

Figure 1. Schematic representation of strategies toward low-energy stiction-free NEM switches utilizing molecular layers. (a) In a conventional contact-based NEM switch, the elastic restoring force should exceed the surface adhesion forces to overcome the energy barrier (ΔE) to break the contact. (b) Low surface energy molecular layers reduce the surface adhesion forces at contact, decreasing the potential for stiction. (c) Additional minimization of stiction can be achieved using a MMM switching gap which further lowers the surface adhesion forces and allows nanoscale force control through compression of the molecular layer, while enabling formation of a few nanometer-thick gap for sub-1 V operation.

while concurrently scaling down the switching gap thickness to just a few nanometers to achieve sub-1 V operating voltages.

The proposed and fabricated MMM structures reported herein form tunneling NEM switches that operate by electrostatic compression of a molecular film sandwiched between conductive contacts. In this squeezable switch, or "squitch," the use of a molecular layer facilitates the formation of a few-nanometer-thick gap between the source and drain electrodes, reducing the mechanical actuation voltage to the sub-1 V regime. The switching mechanism relies on electromechanical modulation of the molecular gap between the electrodes, which allows several orders of magnitude change in the source-to-drain tunneling current. In this geometry, device failure due to wear and adhesion of the electrodes is avoided by eliminating direct contact between the metallic electrodes, minimizing surface adhesion forces and providing nanoscale force control through deformation of the sandwiched molecular film. As the molecular layer is deformed, reducing the electrode–electrode tunneling distance, the increasing surface adhesion force is balanced by the increasing elastic restoring force of the compressed molecules. This prevents the permanent adhesion of electrodes and promotes device transition to the off-state as the applied voltage is removed. To demonstrate the feasibility of this approach for use in low power electronics, we first numerically analyzed the performance of NEM squitches in terms of actuation voltage, switching energy, and switching speed. We then explored the feasibility of the proposed tunneling switching mechanism through preliminary experiments utilizing designs with metal–molecule–graphene tunneling junctions.

DEVICE DESIGN

The main component of the squitch consists of a compressible insulating molecular film sandwiched between conductive contacts (source and drain) to generate a MMM tunneling junction, as shown in Figure 1c. While this schematic shows a vertically actuated device, the same concept can be applied to a laterally actuated squitch.[14] The thickness of the molecular layer defines the charge tunneling distance, and switching is controlled by electromechanical modulation of the tunneling current through the nanometer-scale-thick organic film. As the molecular layer is compressed, the decrease in the tunneling distance is expected to result in an exponential increase in the source-to-drain current,[15] hence turning on the switch. The extent of compression, and in turn the electrical conduction through the thin film, can be controlled by adjusting the applied voltage and is dependent on the electrical and mechanical properties of the molecular layer.

For the squitch system, the organic layer should be an insulating compressible molecular layer whose thickness can be reproducibly controlled at the nanoscale. One promising approach to consistently achieve nanoscale-thick molecular films is molecular self-assembly. Through organic synthesis, these molecular layers can be engineered to adhere to the desired electrode surface and have customizable mechanical properties. The thickness of the switching gap is controlled by the size of the self-assembled molecular film, which can also be modulated through chemical synthesis. The conduction mechanism through molecular junctions has been previously studied by various groups, particularly for SAMs of alkanethiols and dithiols that form on gold (Au) surfaces. Devices containing alkanedithiols, which have a large energy gap of about 8–10 eV[16–18] between the highest occupied molecular orbital (HOMO) and the lowest unoccupied molecular orbital (LUMO), exhibit direct tunneling.[19–21] Although, as our analysis will show, the mechanical properties of alkanedithiol SAMs are not, in fact, suitable for low-voltage squitch operation, we

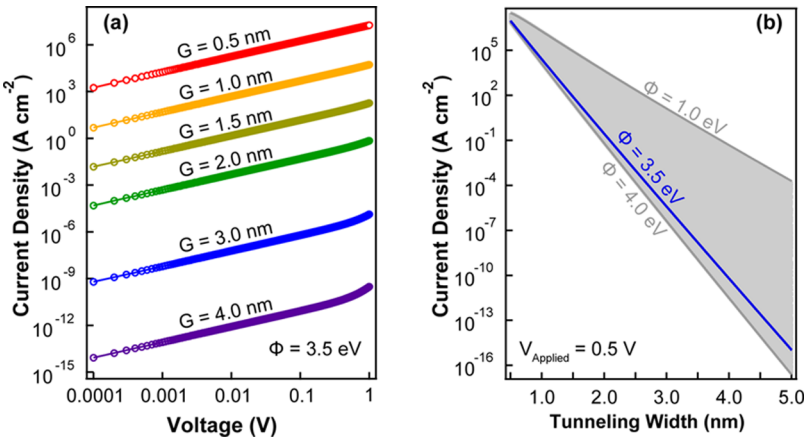

Figure 2. Tunneling current−voltage characteristics of a two-terminal MMM squitch based on the Simmons model. (a) The tunneling current through a molecular film between two Au electrodes as a function of applied voltage at different tunneling widths, *G*, and with α = 0.57 and Φ = 3.5 eV. (b) The exponential dependence of tunneling current on tunneling width at $V_{applied}$ = 0.5 V, α = 0.57, and Φ ranging from 1.0 to 4.0 eV.

envision that their electronic properties resemble those desirable for squitch application. Thus, for the following analysis, the squitch molecular layer is assumed to have electronic properties similar to those of the alkanedithiols in the resting state, while the mechanical properties required for the active layer are investigated. The results of our computational analysis can then be used as a guide toward synthesizing SAMs with the necessary properties to achieve sub-1 V NEM switches.

RESULTS AND DISCUSSION

Electrical conduction through a molecular layer between two metallic plates in the direct tunneling regime ($V < \Phi/q$) can be described using the Simmons model (eq 1):[18,20−23]

$$I = \left(\frac{qA}{4\pi^2\hbar G^2}\right)\left\{\left(\Phi - \frac{qV}{2}\right)\exp\left[-\frac{2(2m)^{1/2}}{\hbar}\alpha\left(\Phi - \frac{qV}{2}\right)^{1/2}G\right] - \left(\Phi + \frac{qV}{2}\right)\exp\left[-\frac{2(2m)^{1/2}}{\hbar}\alpha\left(\Phi + \frac{qV}{2}\right)^{1/2}G\right]\right\} \quad (1)$$

where *A* is the area of the metallic contact, *m* and *q* are the electron mass and charge respectively, ħ is the Planck constant divided by 2π, *G* is the distance between the two electrodes determining the tunneling distance, *V* is the applied voltage, Φ is the energy-barrier height encountered by an electron tunneling through the molecular layer, and α is an adjustable parameter that accounts for the effects of barrier shape and electron effective mass.

Different values of Φ and α have been reported for self-assembled molecular layers depending on the specifics of the molecular junction defined by the type of the molecules, the conductive contacts, and the fabrication method utilized.[18,20,21] Based on measurements of nanotransfer-printed MMM junctions which resemble the vertical structure depicted in Figure 1c, Niskala et al.[21] reported values of Φ ∼ 3.5 eV and α ∼ 0.57 for thiolated alkane molecules. Using these values for Φ and α, the expected terminal current−voltage characteristics as a function of tunneling distance (*G*) are plotted in Figure 2a. Figure 2b highlights the exponential dependence of the tunneling current on *G*, for a given *V* and different values of Φ. This exponential dependence is key to achieving the large on−off current ratio needed for an effective switch. The larger values of Φ lead to a steeper change of tunneling current as a function of *G*, corresponding to a larger on−off current ratio within a smaller range of molecular compression. Thus, a larger Φ achieved through engineering of the molecular layer and the tunneling junction energy level alignment can facilitate fabrication of a squitch with a steep current-switching behavior (Figure 2b).

The tunneling distance in the initial and compressed states determines the current on−off ratio. To ensure a near-zero off-state current, the initial thickness of the molecular layer must be large enough to eliminate any significant tunneling at the desired operating voltage. However, as the material is compressed, the on-state should allow a significant current flow. Based on Figure 2, a 50% compression of the material with Φ = 3.5 eV from *G* = 3 to 1.5 nm results in approximately 7 orders of magnitude change in conduction. The large on−off ratio, due to just 1.5 nm compression, is comparable in performance to high-quality electronic switches. Therefore, in the following analysis, we will assume an archetypical squitch with Φ = 3.5 eV and electrode distance changing from *G* = 3 nm in the off-state to *G* = 1.5 nm in the on-state (Figure 1c). The squitch is also assumed to have lateral dimensions of 100 × 100 nm with 50 nm-thick gold electrodes, feature sizes that can be fabricated using currently available technologies.

In the proposed squitch, the compressive force is provided by an applied electric field between the opposing electrodes sandwiching the molecular layer.

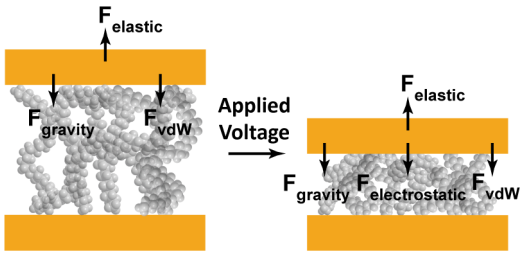

Figure 3. Force balance for a two-terminal squitch: In the off-state the molecular layer elastic force $F_{elastic}$ balances the force of gravity due to the mass of the top electrode ($F_{gravity}$) and the van der Waals force (F_{vdW}) between the electrodes. The electrostatic force, $F_{electrostatic}$, imposed by an applied voltage contributes to F_{vdW} to overcome $F_{elastic}$ to switch on the device.

In a vertically actuated structure, the force of gravity due to the mass of the top electrode (~10 fg) will negligibly contribute to the compression of the thin film; for a laterally actuated structure it is not relevant. Considering the nanometer-scale dimension of the tunneling gap, the presence of Casimir and van der Waals forces between the electrodes must also be considered. Casimir force is quantum mechanical in nature and due to the fluctuations of the electromagnetic field confined in the cavity formed between the metallic plates,[24] while the short-range van der Waals force arises due to fluctuations of the dipole moments in the material.[25,26] Previously, theoretical and experimental investigations have analytically modeled the dependence of these forces on the electrode–electrode gap distance.[27−30] For larger gaps, typically beyond approximately 10% of the metallic plate plasma wavelength (λ_p),[30] it is expected that the Casimir force (with a G^{-4} dependence) will be the dominant attractive force between the plates, while at gaps smaller than this threshold the van der Waals force (with a G^{-3} dependence)[31] will dominate. This suggests that in the MMM squitch that we are modeling with Au electrodes and gaps smaller than 3 nm, considering $\lambda_p \sim 136$ nm[30,32] for an ideal Au film, only van der Waals forces need to be considered as the dominant attractive surface forces.

To compress the molecular film, the electrostatic force due to the applied voltage, $F_{electrostatic}$, and the van der Waals force, F_{vdW}, must overcome the elastic restoring force, $F_{elastic}$, characteristic of the material. Figure 3 shows the simplified lumped model employed to analyze switching speed and energy performance for the two-terminal squitch. In this model, the dynamic equation of motion for the two-terminal device balances electrostatic, elastic, and van der Waals forces ($F(z) = m\,d^2z/dt^2 = F_{electrostatic} + F_{vdW} - F_{elastic}$) which can be expressed as eq 2:

$$m\frac{d^2z}{dt^2} = \frac{\varepsilon_r\varepsilon_0 AV^2}{2(G_o - z)^2} + \frac{A_H A}{6\pi(G_o - z)^3} - k(L - G_o + z) \quad (2)$$

where L is the thickness of the uncompressed molecular film, G_o is the distance between the electrodes when the device is off, which is less than L, since F_{vdW} between metal electrodes results in some compression of the molecular layer, z is the reduction in the tunneling distance (G_o) due to the compression of the molecular layer induced by an applied voltage, A is the device area, ε_0 is the permittivity of free space, ε_r is the dielectric constant of the insulating molecular layer, k is the spring constant that is dependent on the material's Young's modulus, Y, by $k = YA/L$, and A_H is the Hamaker constant. The relative permittivity of the organic material in the squitch is assumed to be 2.1, within the range of values reported for alkanedithiols.[18,33] The Hamaker constant is taken to be 3×10^{-19} J, the approximate value reported in literature.[30] For the following analysis, the molecular layer is modeled as a linear spring with a spring constant independent of the compression while assuming abrupt stiffening upon 1.5 nm displacement, such that compression beyond this point is not allowed. In an actual fabricated system, it is more likely that gradual material hardening is observed during compression with dynamics specific to the material type. Engineering of the properties of the molecular film allows controlled modulation of the tunneling gap to achieve the desired switching characteristics.

An important challenge in the field of electromechanical switches is to minimize their actuation voltages to a range comparable to the current CMOS technologies. To maintain stability during squitch operation, the elastic restoring force provided by the compressed molecular layer should exceed the van der Waals force while being less than the combined van der Waals and applied electrostatic forces to enable device actuation ($F_{vdW} < F_{elastic} < [F_{vdW} + F_{electrostatic}]$). The assumed values of A_H and Y set the magnitude of F_{vdW} and $F_{elastic}$, respectively. The minimum voltage required to actuate a MMM squitch is considered to be the pull-in voltage; at this voltage, the top electrode is displaced to a gap beyond which the combined electrostatic and van der Waals forces overwhelm the elastic force ($F_{elastic} \leq [F_{vdW} + F_{electrostatic}]$) and the top electrode readily accelerates toward the bottom. The pull-in process further contributes to achieving the abrupt switching behavior characteristic of electromechanical systems. Figure 4 shows that the minimum actuation voltage of a MMM squitch can be decreased by using compressible molecular layers with lower Young's moduli. However, the minimum value of the Young's modulus is set by ensuring that upon removal of the applied voltage, the spring force of the compressed molecular layer can overcome the van der Waals force in order to recover the tunneling junction back to its original thickness and turn off the switch. Setting $F_{vdW} \leq F_{elastic}$ at $G = 1.5$ nm suggests that the molecular layer used in the device should

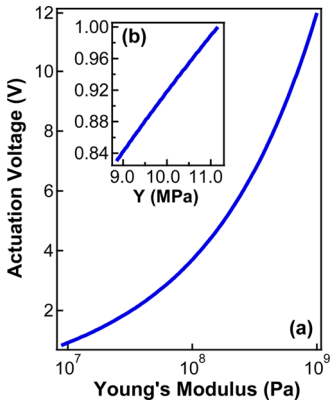

Figure 4. (a) Actuation voltage of the MMM squitch described in the text as a function of Young's modulus of the constituent compressible molecular film. (b) To achieve sub-1 V actuation, a material with Young's modulus <11 MPa is desired.

have $Y \geq 8.9$ MPa for the switch to operate reversibly. Assuming a molecular layer with $Y = 8.9$ MPa, the two-terminal device considered here will actuate at a voltage of 0.83 V, allowing modulation of the tunneling gap from 3 to 1.5 nm to achieve an on−off ratio of 10^7 with an on-state resistance of ~58 MΩ for the 0.01 μm^2 device contact area. The on-state resistance of the device can be lowered by adjusting the device area, the tunneling barrier of the MMM structure, or the width of the on- and off-state gaps, however, the trade-off between these parameters, the on−off ratio, and the actuation voltage must be simultaneously optimized to achieve the desired performance. To operate in the sub 1-V regime, as shown in Figure 4b, an organic layer with $Y < 11$ MPa is necessary, setting a narrow range of $8.9 < Y < 11$ MPa for the molecular film. By engineering the Hamaker constant to lower values, F_{vdW} would be reduced, which would consequently lower the minimum value of Y and further reduce the minimum actuation voltage. For example, a 10-fold reduction in A_H would lead to a 3-fold decrease in the actuation voltage, yielding a 0.26 V squitch.

The switching energy of a squitch is estimated as the total energy associated with charging and discharging of the capacitor formed by the metal electrodes ($E = CV^2$) and compression and relaxation of the molecular spring ($E = kz^2$) in each switching cycle, where C is the capacitance of the tunneling junction in the on-state, V is the actuation voltage, k is the spring constant, and z is the full extent of the molecular layer's compression. In this analysis, it is assumed that the expended energy in one switching cycle is not harnessed toward useful work to promote further switching operations. As shown in Table 1, a squitch based on $Y = 8.9$ MPa molecular film requires 0.15 fJ switching energy.

The squitch switching time is defined to be the time needed for the molecular layer to compress from 3 to 1.5 nm (turning on the switch) in response to the applied voltage, plus the time needed for the material to restore back to its original relaxed state (to turn off the switch) after the applied voltage is removed. To determine the compression time, the nonlinear dynamic equation of motion (eq 2) is solved for a given Y and the corresponding actuation voltage. After the applied voltage is removed, the compressed molecular layer relaxes to turn off the device, modeled as the oscillatory damping of a mass-spring oscillator system toward the off-state position. The relaxation to the off-state is dependent on the properties of the molecular layer utilized. Here, the switch opening time is determined as 1/4 the oscillation period, giving an estimate of the fastest switching time possible in the absence of any external mechanisms to assist the relaxation process. Taking into account material relaxation, the switching time is expected to be marginally slower and material dependent. We anticipate limitations in relaxation time can be overcome by using alternative device designs such as utilizing an extra electrode to assist recovery of the material to the off-state. For the simulated $Y = 8.9$ MPa squitch, the estimated switching time of 6.2 ns at a 0.83 V actuation voltage is among the fastest reported to date for NEM switch technologies.[1−3] Note that the switching speed could also be improved by replacing the Au top electrode with a lighter conductor, such as a graphene membrane, hence reducing the electrode mass. For example, a 16-fold reduction in the top electrode's mass would result in a 4-fold reduction in the switching time.

TABLE 1. Calculated Performance Parameters of a Two-Terminal Squitch As a Function of Young's Modulus of the Molecular Layer

Y (MPa)	$V_{actuation}$ (V)	$E_{switching}$ (fJ)	t_{on} (ns)	t_{off} (ns)	$t_{switching}$ (ns)
8.9	0.83	0.15	2.7	3.5	6.2
10	0.92	0.18	2.4	1.7	4.1
100	3.7	2.4	0.59	0.28	0.87
1000	12	25	0.18	0.085	0.27

The actuation voltages, switching times, and switching energies for the simulated two-terminal MMM squitch are tabulated as a function of Young's modulus in Table 1. These data show a clear trade-off between lower operating voltage and switching speed that must be optimized for the desired application. With $Y \sim$ few MPa, even in the simplest two-terminal device design, sub-1 V and ns-scale operation is possible. In another operation regime, sub-ns actuation is possible when a stiffer molecular film and thus a higher actuation voltage is employed.

Given the MPa Young's moduli constraints for optimal sub-1 V squitch performance, traditional alkanethiol SAMs are not a suitable organic material as the well-packed films exhibit Young's moduli in

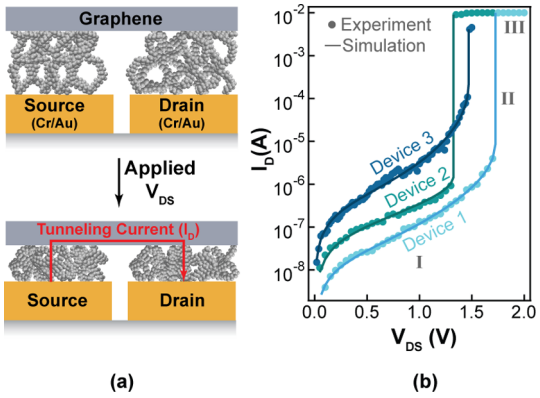

Figure 5. (a) A two-terminal squitch architecture fabricated with interdigitated Au bottom electrodes, self-assembled PEG-dithiol molecular layer, and transferred CVD graphene top electrode. A drain-source voltage (V_{DS}) is applied to decrease the molecular gap and modulate the tunneling current (I_D). (b) Current–voltage characteristics for three example squitches of the design shown in (a) fitted to the theoretically simulated behavior. The following tunneling barrier height, tunneling barrier shape, initial thickness of molecular layer, pull-in gap, dielectric constant, and Young's modulus of molecular layer were used to achieve the simulated best-fit curves: Device 1: Φ = 1.6 eV, α = 0.46, L = 3.1 nm, $G_{pull\text{-}in}$ = 2.2 nm, ε_r = 2.2, Y = 11 MPa; Device 2: Φ = 1.2 eV, α = 0.43, L = 2.2 nm, $G_{pull\text{-}in}$ = 1.6 nm, ε_r = 1.4, Y = 17 MPa; and Device 3: Φ = 4.4 eV, α = 0.41, L = 2.6 nm, $G_{pull\text{-}in}$ = 1.9 nm, ε_r = 2.9, Y = 16 MPa.

the GPa range.[34] Thus, sparsely packed SAMs with significant void space must be investigated to allow for sufficient compression of the material. We envision low Young's moduli SAMs can be achieved through multipodal molecules with "feet" functionalized to adhere to the desired surface,[35,36] molecules with bulky ends to prevent close packing within a monolayer,[37] a combination of long and short alkanes to yield a densely packed base with a sparse top layer,[38] or the use of an entangled polymer film.[39] The requirement of a nanoscale-thick, loosely packed, molecular layer in the squitch is not only a chemistry challenge but also necessitates alternative fabrication techniques. Conventional direct deposition of the electrodes will lead to a low device yield as the void space within the SAM will result in electrical shorting. One approach is to deposit the top electrode of a vertical structure by nondamaging methods, such as nanotransfer-printing of a metal electrode[21] or transfer of an atomically smooth graphene layer.[40] Alternatively, laterally actuated molecular tunneling junctions[14,41] can be fabricated in which the organic molecules are introduced only after patterning of all the electrodes is completed.

To explore the feasibility of the proposed squitch design and tunneling switching mechanism, we fabricated a concept design of squitch based on Au–molecule–graphene tunneling junctions as shown in Figure 5a. The tunneling junction uses interdigitated Au bottom electrodes to form the source and drain contacts. The molecular spacer comprises poly(ethylene glycol)-dithiol (PEG-dithiol) self-assembled onto the Au electrodes. The polymeric self-assembled layer is selected to achieve a sparsely packed molecular film with a lower effective Young's modulus to enable electromechanical modulation of the gap. PEG-dithiol of molecular weight 2000 g/mol is chosen to achieve the desired initial switching gap thickness in the sub-5 nm regime. The top electrode is a graphene sheet synthesized through chemical vapor deposition (CVD) and transferred onto the molecular film. We found that graphene transferred onto the PEG-dithiol layer facilitates the formation of well-defined tunneling gaps with minimal damage to the molecular film compared to the direct deposition of a top metallic contact. Unlike direct deposition which can cause metal penetration through the porous nanometer-thin molecular film, the additive process of transferring CVD graphene electrode with relatively smooth topography results in higher device yield. Hence, for an initial experimental demonstration of the squitch concept, we utilized a graphene top electrode. Figure S1 shows atomic force microscope images of the transferred CVD graphene. It should be noted that despite local smooth topography, the graphene exhibits higher roughness over larger areas due to the roughness of the copper foil used in the growth process and the wrinkles produced through the transfer. This roughness can influence the device reproducibility and stability and can contribute to the variations in performance between different devices. Thus, to realize the squitch's optimal performance and enhance the fabrication yield, further improvements in the graphene transfer process are necessary.

The measured current–voltage characteristics of three such squitches with Au–PEG–graphene designs are shown in Figure 5b. Two operating regimes are observed for these devices. An increase in applied drain-source voltage (V_{DS}) results in an initial exponential increase in the drain current (I_D) followed by an abrupt jump. Region I corresponds to the operating regime prior to pull-in when current increases exponentially as the tunneling gap is reduced by electrostatically induced compression of the molecular layer. On reaching the pull-in distance where the combined electrostatic and van der Waals forces overwhelm the elastic restoring force of the molecular layer, acceleration toward the bottom electrode leads to an abrupt decrease in the tunneling gap and an abrupt increase in current (Region II). The devices presented here exhibit sub-2 V pull-in voltages. The increase in current upon pull-in is limited either by mechanical properties of the material due to stiffening or the measurement instrument compliance (Region III). The differences in performance among devices may be attributed to variations in molecular layer thickness and packing density, roughness of the electrode, which may result in variations in the effective thickness of the switching gap, as well as the properties of the Au–molecule or graphene–molecule

junctions. Additional squitch $I-V$ characteristics and their analyses are included in Figure S2 of the Supporting Information.

To further investigate the current conduction mechanism observed, the experimental data are fitted against the simulated performance. Taking the point of sudden increase in I_D as pull-in, the pull-in voltage in each device is utilized to extract the expected tunneling gap change with an applied V_{DS} by solving the equation of motion (eq 2). The evaluated tunneling gaps are then used with the Simmons tunneling model (eq 1) to simulate the expected current modulation. In fitting the experimental data, a Monte Carlo approach is used where the tunneling barrier height (Φ), tunneling barrier shape (α), initial thickness of the molecular film (L), and the point at which pull-in occurs are the unknown parameters selected randomly within a predefined range to simulate the device performance and extract the expected dielectric constant and Young's modulus of the molecular thin film. In this analysis, the Hamaker constant is set to be 3×10^{-19} J. A detailed overview of the simulation technique and analysis is included in the Supporting Information.

The best-fit curves simulated for each device along with the corresponding parameters and extracted material properties are shown in Figure 5b. The close agreement between the simulated and experimental results supports the proposed tunneling switching mechanism of squitches. It should be noted however that due to the large number of unknown parameters present in the model, other combinations of values for α, Φ and L can yield a close fit to the experiment. Nevertheless, within the possible results, combinations of unknown parameters exist that are within physically reasonable bounds while strongly agreeing with experimentally extracted values of ε_r and Y. With α constrained to 0.7 ± 0.3, $\Phi = 3 \pm 2$ eV, and $\varepsilon_r = 3 \pm 2$, the Young's modulus extracted for a self-assembled layer of PEG-dithiol (2000 g/mol) based on the three devices is within the 5 to 40 MPa range (Figure S3). The pull-in gap for these devices is determined to be in the range of 0.71L to 0.74L where L is the initial thickness of the PEG self-assembled layer. A more precise determination of the parameters requires further information regarding the specifics of the tunneling junction, mechanical properties of the molecular layer, and dynamics of molecular layer electromechanical deformation which necessitates further experimentation and development of molecular level metrological tools.

The concept squitches introduced here serve as preliminary efforts toward the demonstration of tunneling current modulation as the main switching mechanism in an electromechanical switch. Development of an optimal squitch with sub-1 V actuation and reliable switching performance requires engineering of molecular layers with tailored mechanical properties, characterization of molecular level electromechanical dynamics, and practical integration of the molecular layer into optimized device geometries. Furthermore, extension of two-terminal squitches to more complex multiterminal designs with gate-control is desired to render them more practical for applications in integrated systems.

CONCLUSIONS

In summary, we proposed, demonstrated, and numerically simulated a NEM switch that operates by electromechanical modulation of tunneling current through a gap defined by a few nanometer-thick organic molecular layer sandwiched between two electrodes. Compression of the molecular layer by an applied electrostatic force reduces the tunneling gap leading to an exponential increase in the tunneling current. The molecular layer facilitates controlled formation of nanoscale switching gaps, minimizing the operating voltage to the sub-1 V regime, which is not feasible in the current contact-based NEM switches. The compressible molecular film also avoids direct contact of the electrodes to minimize surface adhesion forces and provides force control at the nanoscale where the surface adhesion forces are overcome by the elastic restoring force of the deformed molecules, preventing device failure due to stiction. Theoretical analysis of squitches demonstrates the possibility of achieving sub-1 V operation with abrupt switching behavior and nanoseconds switching time. Preliminary experimental results based on Au–molecule–graphene tunneling junctions suggest the feasibility of electromechanical modulation of tunneling current as a potential switching mechanism in NEM switches. Through engineering of the molecular layer and the design of the device structure, the switching characteristics can further be optimized. The quantum tunneling switching mechanism of these NEM devices identifies squitches as a unique device platform that could overcome limitations of current NEM switch technologies, giving rise to multiple applications in the field of low-power electronics.

METHODS

Device Fabrication. To fabricate the tunneling junction, poly(ethylene glycol)-dithiol (PEG-dithiol) with molecular weight of 2000 g/mol is self-assembled onto interdigitated Cr/Au electrodes (20/50 nm film thickness, respectively) using thiol-chemistry. A solution of 5 mM PEG-dithiol in ethanol was prepared inside a N_2-filled glovebox. The Au bottom electrode was placed inside this solution to form a self-assembled PEG-dithiol layer at room

temperature. After 24 h, the substrates were removed from the PEG-dithiol solution, thoroughly rinsed in ethanol, and dried with a stream of N_2. The graphene top electrode was then transferred onto the molecular layer as discussed below. The tunneling junction was then left inside a desiccator to dry for ~2 h.

Graphene Synthesis. The graphene was grown on a copper foil using low-pressure CVD.[42] First, the Cu foil was annealed at 1000 °C for 30 min in the presence of 10 sccm H_2 flow inside a quartz tube. Then, the graphene growth was initiated by increasing H_2 flow rate to 70 sccm and introducing 4 sccm of CH_4. The growth was allowed to complete for 30 min at a chamber pressure of 1.90 Torr. Through this process, high-quality graphene monolayers were achieved.

Graphene Transfer. To transfer the CVD grown graphene monolayer from the Cu foil to the receiving substrate, first poly(methyl-methacrylate) (PMMA) was spin-coated onto one side of the Cu foil and baked at 80 °C for 10 min. The graphene on the back-side of Cu foil was removed with an O_2 plasma etch. The Cu/graphene/PMMA stack was then placed in $FeCl_3$-based copper etchant for 15 min, allowing the copper to dissolve. The remaining graphene/PMMA film was rinsed in DI water, removed from water using the receiving substrate, and dried using a gentle stream of N_2.[43]

Conflict of Interest: The authors declare no competing financial interest.

Supporting Information Available: Surface roughness analysis of transferred CVD graphene using atomic force microscopy, additional current−voltage characteristics of devices, and detailed overview of the procedure used in analysis and fitting of experimental data. The Supporting Information is available free of charge on the ACS Publications website at DOI: 10.1021/acsnano.5b02476.

Acknowledgment. The authors thank Petar Todorović, Wendi Chang, Apoorva Murarka, Trisha Andrew, and Parag Deotare for insightful discussions. This work was supported by the National Science Foundation (NSF) Center for Energy Efficient Electronics Science (E^3S) Award ECCS-0939514. F.N. acknowledges the support of Natural Sciences and Engineering Research Council of Canada (NSERC).

REFERENCES AND NOTES

1. Loh, O. Y.; Espinosa, H. D. Nanoelectromechanical Contact Switches. *Nat. Nanotechnol.* **2012**, *7*, 283–295.
2. Lee, J. O.; Song, Y.; Kim, M.; Kang, M.; Oh, J.; Yang, H.; Yoon, J. A Sub-1-V Nanoelectromechanical Switching Device. *Nat. Nanotechnol.* **2013**, *8*, 36–40.
3. Kim, J.; Chen, Z. C. Y.; Kwon, S.; Xiang, J. Three-Terminal Nanoelectromechanical Field Effect Transistor with Abrupt Subthreshold Slope. *Nano Lett.* **2014**, *14*, 1687–1691.
4. Jang, W. W.; Lee, J. O.; Yoon, J.; Kim, M.; Lee, J.; Kim, S.; Cho, K.; Kim, D.; Park, D.; Lee, W. Fabrication and Characterization of a Nanoelectromechanical Switch with 15-nm-Thick Suspension Air Gap. *Appl. Phys. Lett.* **2008**, *92*, 103110.
5. Feng, X. L.; Matheny, M. H.; Zorman, C. A.; Mehregany, M.; Roukes, M. L. Low Voltage Nanoelectromechanical Switches Based on Silicon Carbide Nanowires. *Nano Lett.* **2010**, *10*, 2891–2896.
6. Qian, Y.; Lou, L.; Tsai, M. J.; Lee, C. A Dual-Silicon-Nanowires Based U-Shape Nanoelectromechanical Switch with Low Pull-in Voltage. *Appl. Phys. Lett.* **2012**, *100*, 113102.
7. Nathanael, R.; Pott, V.; Kam, H.; Jeon, J.; Liu, T. J. K. 4-Terminal Relay Technology for Complementary Logic. *IEEE Int. Electron Devices Meet., Tech. Dig.* **2009**, 223–226.
8. Rueckes, T.; Kim, K.; Joselevich, E.; Tseng, G. Y.; Cheung, C.; Lieber, C. M. Carbon Nanotube-Based Nonvolatile Random Access Memory for Molecular Computing. *Science* **2000**, *289*, 94–97.
9. Yaung, J.; Hutin, L.; Jeon, J.; Liu, T. J. K. Adhesive Force Characterization for MEM Logic Relays with Sub-Micron Contacting Regions. *J. Microelectromech. Syst.* **2014**, *23*, 198–203.
10. Wagner, T. J. W.; Vella, D. Switch On, Switch Off: Stiction in Nanoelectromechanical Switches. *Nanotechnology* **2013**, *24*, 275501.
11. Loh, O.; Wei, X.; Ke, C.; Sullivan, J.; Espinosa, H. D. Robust Carbon-Nanotube-Based Nano-Electromechanical Devices: Understanding and Eliminating Prevalent Failure Modes Using Alternative Electrode Materials. *Small* **2011**, *7*, 79–86.
12. Dadgour, H.; Cassell, A. M.; Banerjee, K. Scaling and Variability Analysis of CNT-Based NEMS Devices and Circuits with Implications for Process Design. *IEEE Int. Electron Devices Meet., Tech. Dig.* **2008**, 1–4.
13. Maboudian, R.; Ashurst, W. R.; Carraro, C. Self-Assembled Monolayers as Anti-Stiction Coatings for MEMS: Characteristics and Recent Developments. *Sens. Actuators, A* **2000**, *82*, 219–223.
14. Niroui, F.; Deotare, P. B.; Sletten, E. M.; Wang, A. I.; Yablonovitch, E.; Swager, T. M.; Lang, J. H.; Bulović, V. Nanoelectromechanical Tunneling Switches Based on Self-Assembled Molecular Layers. Proceedings of the 27th IEEE International Conference on Micro Electro Mechanical Systems, San Francisco, CA, January 26−30, 2014; IEEE: New York, **2014**; pp 1103−1106.
15. Erbe, A.; Blick, R. H.; Tilke, A.; Kriele, A.; Kotthaus, J. P. A Mechanically Flexible Tunneling Contact Operating at Radio Frequencies. *Appl. Phys. Lett.* **1998**, *73*, 3751.
16. Tomfohr, J. K.; Sankey, O. F. Complex Band Structure, Decay Lengths, and Fermi Level Alignment in Simple Molecular Electronic Systems. *Phys. Rev. B* **2002**, *65*, 245105.
17. Salomon, A.; Cahen, D.; Lindsay, S.; Tomfohr, J.; Engelkes, V. B.; Frisbie, C. D. Comparison of Electronic Transport Measurements on Organic Molecules. *Adv. Mater.* **2003**, *15*, 1881–1890.
18. Akkerman, H. B.; Naber, R. C. G.; Jongbloed, B.; van Hal, P. A.; Blom, P. W. M.; de Leeuw, D. M.; de Boer, B. Electron Tunneling through Alkanedithiol Self-Assembled Monolayers in Large-Area Molecular Junctions. *Proc. Natl. Acad. Sci. U.S.A.* **2007**, *104*, 11161–11166.
19. Holmlin, R. E.; Haag, R.; Chabinyc, M. L.; Ismagilov, R. F.; Cohen, A. E.; Terfort, A.; Rampi, M. A.; Whitesides, G. M. Electron Transport through Thin Organic Films in Metal-Insulator-Metal Junctions Based on Self-assembled Monolayers. *J. Am. Chem. Soc.* **2001**, *123*, 5075–5085.
20. Wang, W.; Lee, T.; Reed, M. A. Mechanism of Electron Conduction in Self-Assembled Alkanethiol Monolayer Devices. *Phys. Rev. B* **2003**, *68*, 035416.
21. Niskala, J. R.; Rice, W. C.; Bruce, R. C.; Merkel, T. J.; Tsui, F.; You, W. Tunneling Characteristics of Au-Alkanedithiol-Au Junctions Formed *via* Nanotransfer Printing (nTP). *J. Am. Chem. Soc.* **2012**, *134*, 12072–12082.
22. Simmons, J. G. Generalized Formula for the Electric Tunnel Effect between Similar Electrodes Separated by a Thin Insulating Film. *J. Appl. Phys.* **1963**, *34*, 1793–1803.
23. Simmons, J. G. Electric Tunnel Effect between Dissimilar Electrodes Separated by a Thin Insulating Film. *J. Appl. Phys.* **1963**, *34*, 2581–2590.
24. Casimir, H. B. G. On the Attraction between Two Perfectly Conducting Plates. *Proc. K. Ned. Akad. Wet.* **1948**, *51*, 793–795.
25. London, F. The General Theory of Molecular Forces. *Trans. Faraday Soc.* **1937**, *33*, 8–26.
26. Dzyaloshinskiĭ, I. E.; Lifshitz, E. M.; Pitaevskiĭ, L. P. The General Theory of van der Waals Forces. *Adv. Phys.* **1961**, *10*, 165–209.
27. Lifshitz, E. M. The Theory of Molecular Attractive Forces between Solids. *Sov. Phys. JETP* **1956**, *2*, 73–83.
28. Casimir, H. B. G.; Polder, D. The Influence of Retardation on the London-van der Waals Forces. *Phys. Rev.* **1948**, *73*, 360–372.
29. Rodriguez, A. W.; Capasso, F.; Johnson, S. G. The Casimir Effect in Microstructured Geometries. *Nat. Phot.* **2011**, *5*, 211–221.
30. Palasantzas, G.; van Zwol, P. J.; De Hosson, J. T. M. Transition from Casimir to van der Waals Force between Macroscopic Bodies. *Appl. Phys. Lett.* **2008**, *93*, 121912.

31. Maboudian, R.; Howe, R. T. Critical Review: Adhesion in Surface Micromechanical Structures. *J. Vac. Sci. Technol. B* **1997**, *15*, 1–20.
32. Lambrecht, A.; Reynaud, S. Casimir Force between Metallic Mirrors. *Eur. Phys. J. D* **2000**, *8*, 309–318.
33. Rampi, M. A.; Schueller, O. J. A.; Whitesides, G. M. Alkanethiol Self-Assembled Monolayers as the Dielectric of Capacitors with Nanoscale Thickness. *Appl. Phys. Lett.* **1998**, *72*, 1781–1783.
34. DelRio, F. W.; Jaye, C.; Fischer, D. A.; Cook, R. F. Elastic and Adhesive Properties of Alkanethiol Self-Assembled Monolayers on Gold. *Appl. Phys. Lett.* **2009**, *94*, 131909.
35. Chen, K. Y.; Wezenberg, S. J.; Carroll, G. T.; London, G.; Kistemaker, J. C. M.; Pijper, T. C.; Feringa, B. L. Tetrapodal Molecular Switches and Motors: Synthesis and Photochemistry. *J. Org. Chem.* **2014**, *79*, 7032–7040.
36. Mann, J. A.; Dichtel, W. R. Improving the Binding Characteristics of Tripodal Compounds on Single Layer Graphene. *ACS Nano* **2013**, *7*, 7193–7199.
37. Lahann, J.; Mitragotri, S.; Tran, T.; Kaido, H.; Sundaram, J.; Choi, I. S.; Hoffer, S.; Somorjai, G. A.; Langer, R. A Reversibly Switching Surface. *Science* **2003**, *299*, 371–374.
38. Chen, S.; Li, L.; Boozer, C. L.; Jiang, S. Controlled Chemical and Structural Properties of Mixed Self-Assembled Monolayers of Alkanethiols on Au(111). *Langmuir* **2000**, *16*, 9287–9293.
39. Unsworth, L. D.; Tun, Z.; Sheardown, H.; Brash, J. L. Chemisorption of Thiolated Poly(ethylene oxide) to Gold: Surface Chain Densities Measured by Ellipsometry and Neutron Reflectometry. *J. Colloid Interface Sci.* **2005**, *281*, 112–121.
40. Suk, J. W.; Kitt, A.; Magnuson, C. W.; Hao, Y.; Ahmed, S.; An, J.; Swan, A. K.; Goldberg, B. B.; Ruoff, R. S. Transfer of CVD-Grown Monolayer Graphene onto Arbitrary Substrates. *ACS Nano* **2011**, *5*, 6916–6924.
41. Niroui, F.; Sletten, E. M.; Deotare, P. B.; Wang, A. I.; Swager, T. M.; Lang, J. H.; Bulović, V. Controlled Fabrication of Nanoscale Gaps Using Stiction. Proceedings of the 28th IEEE International Conference on Micro Electro Mechanical Systems, Estoril, Portugal, January 18−22, 2015; IEEE: New York, **2015**; pp 85−88.
42. Li, X.; Cai, W.; An, J.; Kim, S.; Nah, J.; Yang, D.; Piner, R.; Velamakanni, A.; Jung, I.; Tutuc, E.; et al. Large-Area Synthesis of High-Quality and Uniform Graphene Films on Copper Foils. *Science* **2009**, *324*, 1312–1314.
43. Reina, A.; Jia, X.; Ho, J.; Nezich, D.; Son, H.; Bulović, V.; Dresselhaus, M. S.; Kong, J. Large Area, Few-Layer Graphene Films on Arbitrary Substrates by Chemical Vapor Deposition. *Nano Lett.* **2009**, *9*, 30–35.